

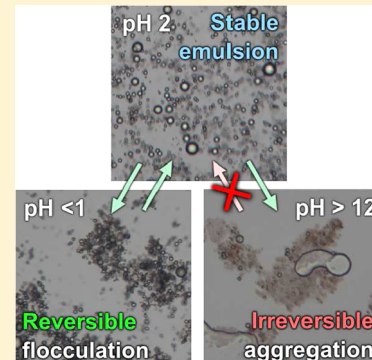


Graphene Oxide-Stabilized Oil-in-Water Emulsions: pH-Controlled Dispersion and Flocculation

Thomas M. McCoy, Matthew J. Pottage, and Rico F. Tabor*

School of Chemistry, Monash University, Clayton, VIC 3800, Australia

ABSTRACT: Oil-in-water emulsions stabilized by graphene oxide (GO) can be flocculated by either an increase or a decrease in pH. At highly acidic pH, fully reversible flocculation of emulsion droplets can be achieved, whereas when adjusted to high pH, the flocculation is irreversible, which we interpret as a permanent chemical change in the GO. We correlate the effectiveness of GO as a stabilizer to its aqueous aggregation state and explore the effects of the GO surface charge in determining emulsion properties. By directly measuring the interaction forces between two emulsion droplets coated in GO using the atomic force microscope, we demonstrate the basis for the pH-dependent flocculation behavior. It is shown that interfacial charge of the GO and oil–water interface is the overriding drive for the exceptional stability of acidic GO emulsions.



INTRODUCTION

The unique water dispersibility and ease of manufacture of graphene oxide (GO) make it an appealing material for many applications where pristine graphene is not suitable,^{1,2} including sensors,³ adsorbents, and dispersants.⁴ Of increasing interest is the ability of GO to adsorb at, and stabilize, air–water and oil–water interfaces.^{4–6} Current models suggest that GO sheets bear hydrophilic carboxyl groups around their periphery and a hydrophobic basal plane.¹ The carboxyl functionalities can be deprotonated to yield charged groups, offering a considerable contrast in polarity with the broadly hydrophobic “faces” of the sheets. This amphiphilic nature goes some way to explaining the propensity of GO to locate at interfaces.

Because of its heterogeneous structure and the fact that its chemistry can depend on the synthesis and preparation route, GO exhibits complex physical and chemical behavior. There is evidence that it can exhibit both molecular and particle-like properties, depending on solution conditions. For example, Shih et al. found that GO was surface-active (that is, it reduced the surface tension of water) at pH 1, but not at pH 14, citing a difference in effective hydrophobicity due to protonation and deprotonation of the edge carboxyl groups.⁷ Molecular modeling showed that GO tends to form sandwich-like complexes, which are surface-active at pH 1 but not at pH 14. They also posited that despite its apparent amphiphilicity, GO did not micellize at either pH studied. The same pH-dependent effect on interfacial tension for GO at the toluene/water interface was shown previously by Kim et al.⁴ However, other researchers have noted that GO can still stabilize emulsions at high pH values⁶ and that the GO may undergo a chemical change at high pH that results in reduced oxygen functionality on the sheets. As interfacial tension is not affected by GO adsorption in this case, it can be considered that GO is behaving as a particle, and thus the oil–water emulsions

generated from its dispersion are of the Pickering or Ramsden (particle-stabilized) type.⁸ This also raises the important question of whether GO adsorption in basic conditions is spontaneous, as is seen in acidic conditions. Like a particle, it has been shown that GO adsorption at the air–water interface can be enhanced by flotation using gas bubbles.⁵

The acid–base chemistry of GO along with its charging behavior are predicated on its organic origins, where it is seen to behave as a moderate-strong acid, remaining negatively charged to pH 1 and below.^{7,9,10} Recent work has attempted to explain this unusual characteristic by examining the contributions from the pK_a of the detected oxygen-containing groups on the GO sheets.¹¹ The role of oxidative debris from GO synthesis has also been implicated in the strong pH dependence of the material, whereby smaller, highly oxidized organic fragments are purported to stabilize the GO sheets.^{12,13}

The formulation of GO-stabilized oil-in-water emulsions has been examined recently, including the effects of pH, added salt,¹⁴ and reduction of the GO.⁶ In general, the emulsions display remarkable stability when compared to those stabilized by typical molecular surfactants. Because of the complex chemical nature of the GO, a range of unusual behavior is seen in these systems including formation of nonspherical droplets.⁶ However, the physical and chemical basis for the properties of these emulsions is not yet fully understood.

Theoretical calculations have also been used to understand the complex chemical and physical properties of GO, exploring properties such as its surface chemistry, electronic structure, and reactivity¹⁵ as well as its aggregation and interactions with water.⁷

Received: January 3, 2014

Revised: February 4, 2014

Published: February 5, 2014

Here, we directly probe the origins of the pH dependence of emulsions stabilized by GO, by measuring the interaction forces between emulsion droplets using the atomic force microscope. We observe microscopically that at high and low pH flocculation of otherwise stable GO emulsions is achieved and that at highly basic conditions this flocculation is irreversible. The effects of the surface charge on the GO sheets are determined by measuring their adsorption at oil–water interfaces and also at a model hydrophobic interface—gold.

RESULTS AND DISCUSSION

Graphene oxide was synthesized from graphite using a modified Hummers method;¹⁶ particle size and layer thickness were characterized using atomic force microscopy (AFM) imaging, and its aqueous dispersion stability was assessed by dynamic light scattering (Figure 1a,b,d). From substantial AFM imaging

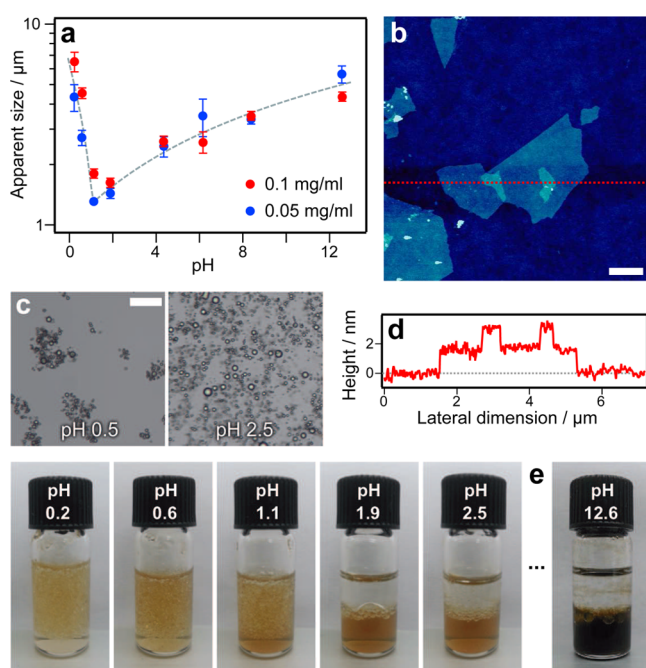


Figure 1. Stability of aqueous GO and GO-stabilized oil-in-water emulsions. (a) Dynamic light scattering data showing the apparent GO particle size as a function of pH for two different dispersion concentrations. The dashed line is drawn as a guide to the eye. (b) AFM height image of GO sheets dried onto glass, showing their typical lateral dimensions. The scale bar represents 1 μm , and the dotted line signifies the sectional height profile presented in (d). (c) Microscopy images of GO emulsions produced by 60 s sonication of 0.5 mL of toluene and 0.5 mL of a 2 mg/mL GO dispersion at different pHs. The scale bar represents 100 μm . (d) Sectional height profile from the AFM image shown in (b). (e) Emulsions generated by vigorous manual shaking of 0.5 mL of toluene and 0.5 mL of aqueous GO dispersion at different pH values. Note that the oil is less dense than the aqueous phase.

of samples adsorbed onto glass substrates, it appeared that complete exfoliation to monolayer GO was obtained, with an average particle size of ca. 2 μm . To assess the ability of the GO to stabilize oil–water interfaces, emulsion samples were prepared comprising toluene and aqueous GO dispersion. Emulsions stabilized by GO could be readily formed by shaking or sonicating the oil with an equal volume of aqueous GO dispersion. As previous experiments have shown,^{4,6} the

formation of these emulsions is heavily influenced by the pH of the aqueous component, with acidic dispersions appearing to form the most stable emulsions. The rationale for this observation is that the carboxyl groups around the periphery of the GO sheets are more dissociated at higher pH, making the material more charged and thus less surface active.⁷

For emulsions formed by vigorous manual shaking, at pH 2.45 and 1.89, only very small emulsion layers were observed, whereas at pH 1.12, 0.57, and 0.22, quite substantial emulsions with very small droplet sizes were formed (Figure 1e). This demonstrates that highly acidic conditions facilitate the formation of GO stabilized oil-in-water emulsions and suggests that complex surface chemical relationships are responsible for this behavior. Microscopic observation of emulsions produced at pH 0.5 and 2.5 by sonication of the shaken samples (Figure 1c) shows that at pH 2.5 droplets are relatively freely dispersed, whereas at pH 0.5, droplets are flocculated together. This flocculation appears to “gel” the emulsion, holding the coated droplets in place and significantly enhancing the stability of the emulsion layer by halting droplet collisions and creaming.

At basic conditions (pH 12.6) almost no emulsion layer was formed by vigorous shaking of toluene and aqueous GO. In addition, the GO itself appeared much darker in color than at lower pH values and formed loose aggregates that could be seen with the naked eye over the course of 1 h, in line with previous reports of the dispersion properties of the material.¹⁷

Dynamic light scattering data obtained of aqueous GO dispersions as a function of pH (Figure 1a) appears to raise further questions. The GO appears to be most stable in solution at around pH 2, as characterized by the lowest effective particle size, which correlates well with the average size seen by AFM imaging. The larger sizes at higher and lower pH values indicate aggregation or flocculation of the GO sheets or attractive interactions between them. The minimal difference between the sizes reported from the two concentrations studied suggests that physical aggregation is the more likely explanation, as concentration-dependent interparticle interactions would likely manifest as a consistent difference in size between the two concentrations. It should be noted that the GO dispersions at low pH values (pH 3) macroscopically flocculate very slowly (over the course of days to weeks). The reason for such slow aggregation may be a combination of low interparticle forces and the remaining surface charge, although this remains to be quantified precisely.

At low pH, this flocculation is explained by condensation of protons to the carboxylate groups, thus reducing the effective surface charge on the particles below the ≈ 30 mV required for charge-based stability of a colloidal dispersion.¹⁸ Then, van der Waals, π -stacking, and hydrophobic interactions, all of which are attractive, dominate. However, at high pH, aggregation is more surprising, as increasing pH should further dissociate carboxyl functionalities and increase charge stability. Previous research has suggested that base can reduce GO comparatively readily,¹⁹ which could also explain the behavior seen here; base has also been implicated in changing the effects of “oxidative debris” within GO systems.^{12,13} We discuss these possibilities in greater detail below.

In order to further explore the interplay of surface charge and other factors on the stability and adsorption characteristics of GO, adsorption at a model hydrophobic interface—in the form of gold—was explored. The charging behavior of gold–water^{20,21} and oil–water^{22,23} interfaces has been well-characterized, and thus we can use gold (which is easy to

image in the AFM) to predict and explore the charge-dependent adsorption of GO at the oil–water interface (which is almost impossible to image directly in the AFM). The work of Creux et al.²² shows that a wide range of chemically different oils show almost identical charging behavior as a function of pH. Figure 2a shows literature values for the surface or zeta potentials of relevant interfaces. Where the surface charge on the GO particles and the adsorbent interface are of different sign, we expect an electrical double-layer attraction between the surfaces and would thus predict strong adsorption. These regions are highlighted for gold–water and oil–water interfaces

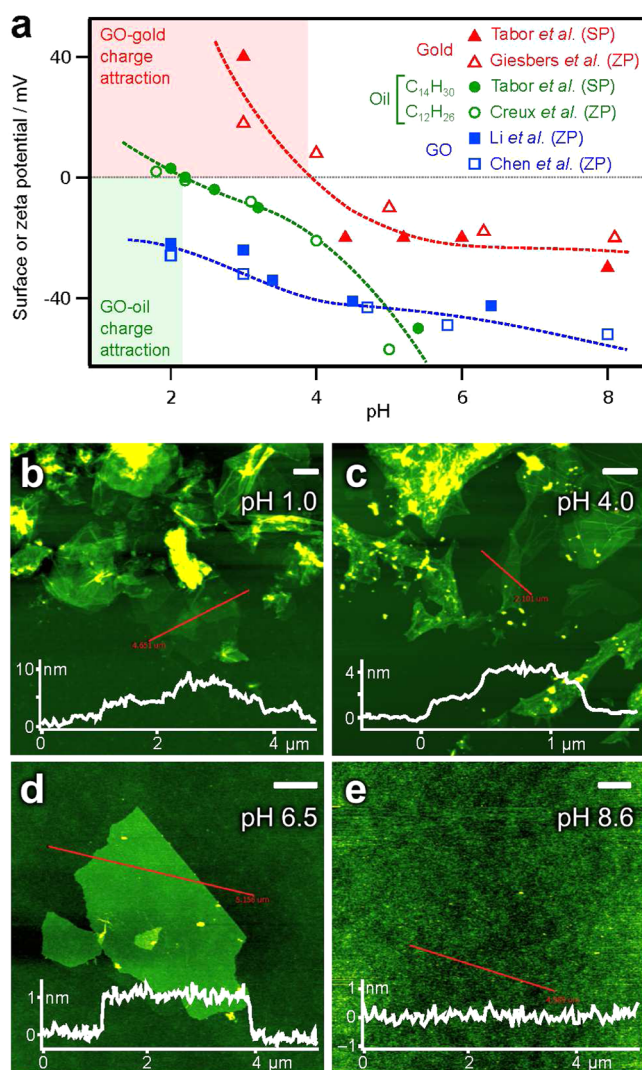


Figure 2. Charge interaction between GO and gold/water and oil/water interfaces. (a) Literature values for the surface or zeta potentials of GO and of the gold/water and oil/water interfaces. Data for gold are from Tabor et al.²¹ and Giesbers et al.;²⁰ for oils (tetradecane and dodecane) from Tabor et al.²³ and Creux et al.;²² for GO are from Li et al.⁹ and Chen et al.¹⁰ Note that “SP” means that a surface potential was measured and “ZP” means that a zeta potential was measured. They are assumed to be approximately equivalent here. The shaded regions show the pH ranges within which GO and gold or GO and oil would be expected to experience an attraction based on their surface charge states. (b–e) AFM height images of GO adsorbed on gold from aqueous dispersion as a function of pH. The inset line profiles show the sample height as a function of lateral coordinate for the lines given in red on each panel. The scale bar in each panel represents 1 μm .

by shading in Figure 2a. A more compelling reason for the enhanced stability of GO emulsions below pH 2 becomes immediately apparent—in this region, the GO and oil–water interface bear opposite charges, and thus strong adsorption would be expected. The electrical double-layer force operates over a significantly larger range than van der Waals or hydrophobic forces,²⁴ and thus the adsorption rate would also be enhanced, explaining the minimal mechanical shaking required for acidic GO dispersions to emulsify oil.

To confirm this supposition, we imaged samples where GO had been adsorbed onto gold surfaces at various pHs, including where a strong charge attraction would be expected (pH 1). As predicted, significant adsorption was seen at pH values at or below the IEP of gold (Figure 2b), where the gold surface is positively charged and the GO remains negatively charged. Conversely, at high pH the GO and the gold both have a negative charge and thus experience a mutual repulsion. At pH 6.48, a 1 nm thick, individual flake of GO was found on the gold surface, and at pH 8.61, virtually nothing adsorbed to the gold surface, which is supported by the subnanometer scale of the line profile, indicating that the surface is extremely flat and lacking in any features.

It is interesting to note that at the lowest pH values aggregated clusters of GO were observed on the surface, confirming the idea that it did not possess sufficient surface charge for colloidal stability and had flocculated significantly before adsorption. Additionally, the adsorption at low pH was of “crumpled” sheets, whereas at higher pH adsorption was much more flat and conformal. A possible explanation is that at high pH the main attractions between the gold surface and GO flakes are the van der Waals and hydrophobic forces,²⁵ operating primarily on the basal plane of the flake; at low pHs, the attraction is dominated by the longer-range charge mechanism that operates on the edges of the flakes. These observations indicate that by careful control of the balance of charge and hydrophobicity, the morphology and adsorption mode of GO can be modulated.

In order to probe the interdroplet interactions in GO emulsions, we directly measured the forces between GO-coated emulsion droplets using the atomic force microscope (AFM), with the experiment shown schematically in Figure 3a. The force of interaction detected during the approach and retract of two GO-coated perfluorohexane droplets is shown in Figure 3b,c, where at large separations droplets are far apart (and thus no interaction is detected by the AFM cantilever) and at close approach the droplets interact with one another and deform. The theory and execution of such measurements between oil droplets have been covered in detail recently.²⁶ A positive force indicates a repulsive interaction, whereas a negative force indicates an attraction or adhesion.

At pH 7, the droplets show a strong double-layer repulsion due to the charged GO particles on their surfaces, and there is no hysteresis between the approach and retract branches (Figure 3c), which indicates that a stable aqueous film is retained between the drops at all times. At pH 4, only a small deviation from this behavior is seen (Figure 3d), whereby on retraction of the two drops from their closest approach, very minor adhesions are seen, suggesting that the GO sheets on the opposing drops interact only slightly with one another; at this pH charge repulsion between the sheets still dominates.

For GO-coated drops at pH 2, the retract branch shows many adhesive contacts between the drops, interpreted as strong interactions between the GO sheets on the two droplets.

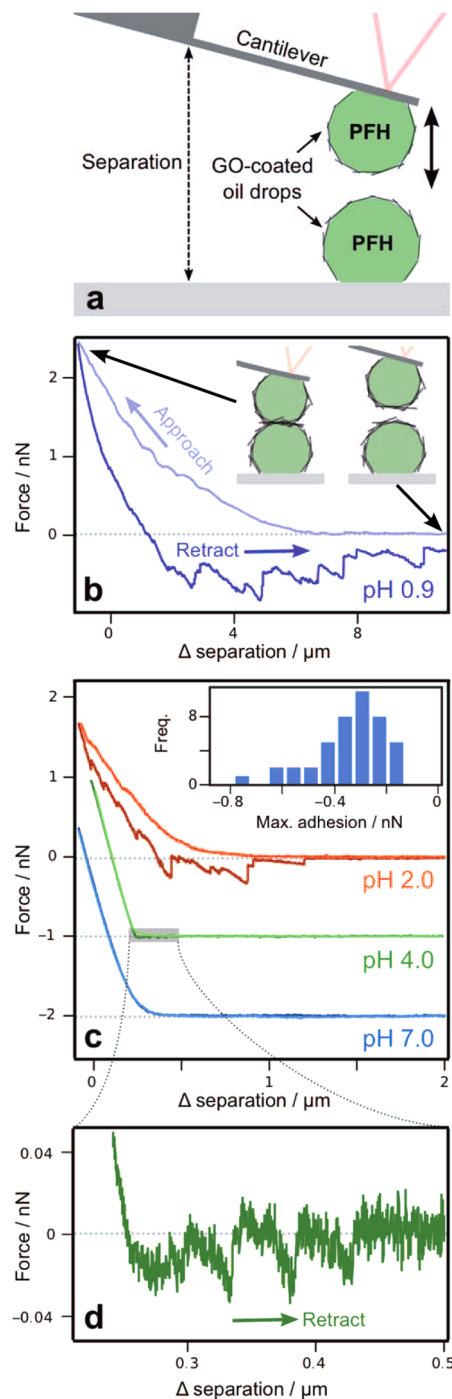


Figure 3. Measured forces between GO-coated oil drops in water. (a) Schematic diagram of the AFM experiment. (b) The measured interaction force between two GO-coated perfluorohexane (PFH) drops (radii 45 and 52 μm) in water at pH 0.9. The y-axis represents force as obtained from the bending of the AFM cantilever, and the x-axis is the change in separation between the back of the cantilever and the substrate, where 0 is arbitrarily defined. The approach branch (top) and retract (bottom) show significant hysteresis, where the jagged adhesions in retraction suggest “detachments” pH values. Note that the traces for pH 4.0 and 7.0 have been offset by -1 and -2 nN, respectively, for clarity. The inset shows a histogram of the maximum force of adhesion between two GO-coated PFH drops in water at pH 2.0, from 44 separate measurements. (d) Zoomed-in view of the retraction region for PFH drops at pH 4 seen in (c) showing very weak detachments.

At pH 2, the surface charge of GO is low and thus can be overcome by the hydrophobic or π -stacking attraction between the sheets, resulting in strong adhesions between the GO particles on the droplets. It is also possible that at close approach, GO sheets can “bridge” between the two droplets themselves. A histogram of the maximum force of adhesion is shown in the inset to Figure 3c. Crudely integrating typical detachment events shows that the associated energy of adhesion ranges between 1×10^{-17} and 1×10^{-19} J, orders of magnitude greater than the typical thermal energy of such droplets at room temperature. This adhesion explains the flocculated, “gelled” appearance and remarkable stability of GO-stabilized emulsions at low pH values, as the drops are effectively immobilized.

At the lowest pH value measured, pH 0.9, the drops are covered with large flocs of GO that interact at very large separations (Figure 3b). It is important to note that at all pHs measured, the droplets were stable to coalescence at the maximum forces applied here. At high (reducing) pH, we were unable to measure interdroplet forces as the droplets tended to detach from the cantilever. This may be due to a change in the gold–thiol chemistry used to hydrophobize the cantilever at these basic conditions.

Having isolated the surface chemical reasons behind the reversible flocculation of GO-stabilized emulsions at low pH, the issue of emulsion behavior at high pH is clearly an outstanding question, with conflicting explanations in the literature. We found that adjusting the pH of a stable, acidic GO emulsion to pH 10 resulted in phase separation (Figure 4); however, readjustment back to pH 0.5 allowed restabilization of the emulsion. Conversely, adjusting the same, initially stable emulsion to pH 12 resulted in a more complete phase separation, which was *not* reversible when the pH was readusted to 0.5. This suggests that at the more basic condition a *permanent chemical change* in the GO is observed that reduces its ability to charge. We thus posit that decarboxylation has taken place. When looking at the microscopic droplets generated by sonication of these coarse emulsions (Figure 4c), it is seen that at highly basic conditions the GO is strongly aggregated and that many drops have coalesced to give larger, coarser oil drops. In addition, many of these drops are nonspherical, suggesting that the GO has a locked configuration at the interface due to very strong interparticle interactions.

We interpret these observations as a permanent reduction of the GO in basic conditions, as the microscopic observation of the droplets generated is in line with those seen for emulsions produced from reduced graphene oxide.⁶ It is also possible that oxidative debris plays a role, although it is less immediately clear how this would lead to the very specific pH-dependent irreversibility seen here.

It is also interesting to note the difference in emulsification between samples generated from unmixed oil and aqueous GO dispersion at high pH and those generated by the addition of base to an already-formulated emulsion. In the former case, almost no emulsion is generated (Figure 1e), whereas for the adjusted emulsion, some stability is retained, particularly for the sonicated emulsion where the interfacial area is much higher (Figure 4c). This suggests that the primary difference is in the spontaneity of adsorption: at acidic pH, GO not only is surface-active but also adsorbs to oil–water⁴ (and air–water⁷) interfaces spontaneously. At basic pH, this adsorption is clearly not spontaneous. Simply shaking oil and basic GO in water will *not* readily produce an emulsion. However, *in situ* modification

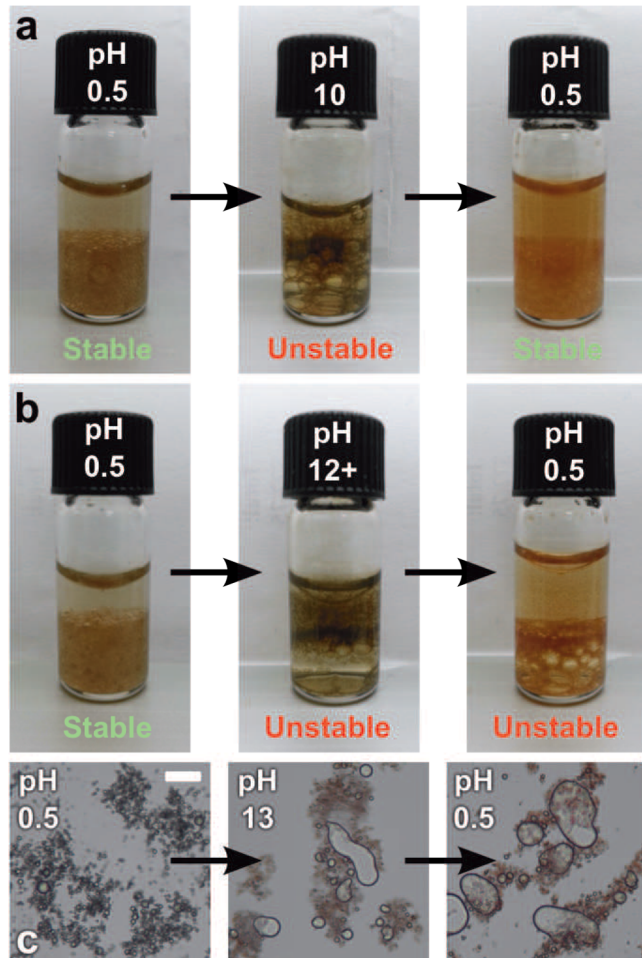


Figure 4. Effects of pH adjustment on GO-stabilized perfluorohexane (PFH)-in-water emulsions. Note that PFH is considerably denser than water, and so o/w emulsion droplets would be expected to form a layer at the bottom of the sample in this case, in contrast to the (light) toluene droplets seen in Figure 1 above which rise to the top. (a) The pH of a stable PFH/water emulsion stabilized by GO and formed by gentle shaking of the vial was adjusted from 0.5 to 10 and back to 0.5. The emulsion was unstable at pH 10, but restabilized at pH 0.5. (b) When the experiment in (a) was performed wherein adjustment of the pH was to 12, readjustment of the pH to 0.5 did *not* restore emulsion stability. (c) Microscopy images of emulsions formed by sonication adjusted from pH 0.5 to 13 and back to 0.5. The scale bar represents 100 μ m.

of the GO surface chemistry when already at the interface will mean that some is desorbed (causing the destabilization seen in Figure 4b and the increased droplet size in Figure 4c), but some remains at the interface in its reduced state.

CONCLUSION

We have demonstrated that GO-stabilized oil-in-water emulsions can be flocculated by moving to either acidic or basic conditions and that a subtle interplay of surface charge and hydrophobicity is responsible for the behavior seen. At low pH, droplet flocculation is fully reversible, whereas at high pH, flocculation is irreversible and appears to be connected with a permanent chemical change in the GO itself. The remarkable increase in stability of GO-stabilized oil-in-water emulsions at acidic pH can be attributed to the charge reversal of the oil–water interface. The resulting strong attraction between the

positively charged interface and negatively charged GO results in rapid, strong adsorption. The same hydrophobic forces that cause flocculation of GO in acidic conditions undoubtedly contribute to this adsorption, as well as flocculating the GO-coated droplets, resulting in a robust, gelled emulsion. By using atomic force microscopy, we directly measured the forces between GO coated drops, demonstrating a physical basis for the robustness of acidic GO emulsions.

The reversible flocculation seen here may have applications in the recovery and recycling of oily wastes from industrial fluids and processing as well as environmental decontamination. These results thus present new methods for the process control of emulsions stabilized by nanomaterials and suggest that surface charge and non-DLVO forces can be used to subtly manipulate the structure and stability of such dispersions.

MATERIALS AND METHODS

Materials. The oils toluene (ChemSupply, Gillman, SA, Australia; reagent grade) and perfluorohexane (Fluorochem, 99%) were used as received. Phosphoric, sulfuric, and hydrochloric acids, potassium hydroxide, and potassium permanganate were from ChemSupply (all 99% or greater) as was hydrogen peroxide solution (30% w/w in water); all were used as received. Mica disks for AFM imaging were from ProSciTech (Thuringowa, QLD, Australia) and were coated with 5 nm of chromium and 50 nm of gold using a Quorum Q150T-S sputter coater.

GO was synthesized from graphite (100 mesh, Sigma-Aldrich) using the modified Hummers method presented by Marcano et al.¹⁶ Graphite powder (1 g) was dispersed in 113 mL of a 9:1 mixture of concentrated sulfuric:phosphoric acids and held at room temperature. Potassium permanganate (6 g) was then added slowly with stirring. The temperature was increased to 50 °C, and the mixture was stirred vigorously for 9 h. The orange/brown reaction mixture was then left to cool to room temperature and poured over ice (ca. 300 mL) with approximately 1 mL of 30% H₂O₂. This mixture was then filtered to remove any large particles and centrifuged at 6000 rpm for 1 h. The supernatant liquid was discarded, and the GO was thrice redispersed in ultrapure water and centrifuged at 6000 rpm for 1 h. The pure GO obtained was then dried at 45 °C.

Methods. Coarse emulsions were prepared by vigorous shaking of equal volumes of oil and aqueous GO dispersion in 1.8 mL vials. Finer emulsions were produced by taking these samples and sonicating in a 100 W ultrasonic bath for 2 min. Polarizing light microscopy (PLM) images were obtained using a CCD camera (Flea3, Point Gray, Richmond, BC, Canada) coupled to a Kozo XJP 300 polarizing microscope.

Dynamic light scattering measurements were made using a Brookhaven ZetaPlus instrument, wherein autocorrelation functions for light scattered at 90° from the incident beam were fitted to obtain particle diffusion coefficients, D , and translated into apparent particle hydrodynamic radii, r_H , using the Stokes–Einstein equation: $r_H = k_B T / 6\pi\eta D$, where k_B is Boltzmann's constant and η is the solvent viscosity.

Atomic force microscopy measurements (imaging and force–separation curves) were made using a JPK Nanowizard 3 AFM. This instrument is equipped with capacitive sensors to ensure accurate reporting of height, z , and x – y lateral distances. Imaging was performed in tapping mode using Bruker NCHV model cantilevers, with nominal resonant frequencies of 340

kHz and spring constants of 20–80 N/m. Images were obtained with a set-point force of 1 nN.

Force measurements between oil drops were made using the standard protocol developed at the University of Melbourne and covered in a recent methods article.²⁶ Briefly, tipless rectangular cantilevers ($450 \times 50 \times 3 \mu\text{m}^3$) were fabricated with a gold disk (diameter $45 \mu\text{m}$) added $\approx 2 \mu\text{m}$ from the free end of the lever.²⁷ This disk was hydrophobized using 1 mM decanethiol in ethanol to provide a surface for droplet attachment. Cantilever spring constants, K_s , were determined by the method of Hutter and Bechhoeffer.²⁸ Perfluorohexane drops were generated by discharging a glass syringe containing the oil underwater into a specially made perfusion cell. The cantilever was brought down onto a suitably sized droplet, which formed a contact region with the hydrophobized disk. This drop was then positioned over another drop, with alignment and axisymmetry ensured using the Nikon Eclipse TE2000 inverted microscope on which the AFM is mounted. GO solution at the desired pH was added using the perfusion cell, and the system was allowed to equilibrate for 30 min. The solution was then exchanged for water set to the same pH, as without this step, free GO scattered the laser used to detect deflection of the AFM cantilever. A force measurement was then performed by bringing the cantilever down until a fixed force had been reached and retracting it. All force measurements were performed at pseudoequilibrium velocities (100 nm/s) to ensure that hydrodynamics did not influence the force behavior.²⁹

AUTHOR INFORMATION

Corresponding Author

*E-mail rico.tabor@monash.edu; Ph +61 3 9905 4558; Fax +61 3 9905 4597 (R.F.T.).

Notes

The authors declare no competing financial interest.

ACKNOWLEDGMENTS

We are indebted to Mainak Majumder, Shannon Notley, and John Texter for insightful discussions concerning 2D nanomaterials.

REFERENCES

- (1) Cheng, C.; Li, D. Solvated Graphene: An Emerging Class of Functional Soft Materials. *Adv. Mater.* **2013**, *25*, 13–30.
- (2) Chen, D.; Feng, H.; Li, J. Graphene Oxide: Preparation, Functionalization, and Electrochemical Applications. *Chem. Rev.* **2012**, *112*, 6027–6053.
- (3) Borini, S.; White, R.; Wei, D.; Astley, M.; Haque, S.; Spigone, E.; Harris, N.; Kivioja, J.; Ryhanen, T. Ultrafast Graphene Oxide Humidity Sensors. *ACS Nano* **2013**, *7*, 11166–11173.
- (4) Kim, J.; Cote, L. J.; Kim, W.; Yuan, F.; Shull, K. R.; Huang, J. Graphene Oxide Sheets at Interfaces. *J. Am. Chem. Soc.* **2010**, *132*, 8180–8186.
- (5) Kim, F.; Cote, L. J.; Huang, J. Graphene Oxide: Surface Activity and Two-Dimensional Assembly. *Adv. Mater.* **2010**, *22*, 1954–1958.
- (6) He, Y.; Wu, F.; Sun, X.; Li, R.; Guo, Y.; Li, C.; Zhang, L.; Xing, F.; Wang, W.; Gao, J. Factors That Affect Pickering Emulsions Stabilized by Graphene Oxide. *ACS Appl. Mater. Interfaces* **2013**, *5*, 4843–4855.
- (7) Shih, C.-J.; Lin, S.; Sharma, R.; Strano, M. S.; Blankschtein, D. Understanding the pH-Dependent Behavior of Graphene Oxide Aqueous Solutions: A Comparative Experimental and Molecular Dynamics Simulation Study. *Langmuir* **2012**, *28*, 235–241.
- (8) Binks, B. P.; Horozov, T. S. *Colloidal Particles at Liquid Interfaces*; Cambridge University Press: Cambridge, UK, 2006.
- (9) Li, D.; Muller, M. B.; Gilje, S.; Kaner, R. B.; Wallace, G. G. Processable Aqueous Dispersions of Graphene Oxide Nanosheets. *Nat. Nanotechnol.* **2008**, *3*, 101–105.
- (10) Chen, J.-T.; Fu, Y.-J.; An, Q.-F.; Lo, S.-C.; Huang, S.-H.; Hung, W.-S.; Hu, C.-C.; Lee, K.-R.; Lai, J.-Y. Tuning Nanostructure of Graphene Oxide/Polyelectrolyte LbL Assemblies by Controlling pH of GO Suspension to Fabricate Transparent and Super Gas Barrier Films. *Nanoscale* **2013**, *5*, 1–7.
- (11) Konkena, B.; Vasudevan, S. Understanding Aqueous Dispersion Ability of Graphene Oxide and Reduced Graphene Oxide through pKa Measurements. *J. Phys. Chem. Lett.* **2012**, *3*, 867–872.
- (12) Rourke, J. P.; Pandey, P. A.; Moore, J. J.; Bates, M.; Kinloch, I. A.; Young, R. J.; Wilson, N. R. The Real Graphene Oxide Revealed: Stripping the Oxidative Debris from the Graphene-like Sheets. *Angew. Chem., Int. Ed.* **2011**, *50*, 3173–3177.
- (13) Thomas, H. R.; Day, S. P.; Woodruff, W. E.; Valles, C.; Young, R. J.; Kinloch, I. A.; Morley, G. W.; Hanna, J. V.; Wilson, N. R.; Rourke, J. Deoxygenation of Graphene Oxide: Reduction or Cleaning? *Chem. Mater.* **2013**, *25*, 3580–3588.
- (14) Yoon, K. Y.; An, S. J.; Chen, Y.; Lee, J. H.; Bryant, S. L.; Ruoff, R. S.; Huh, C.; Johnston, K. P. Graphene Oxide Nanoplatelet Dispersion in Concentrated NaCl and Stabilization of Oil/Water Emulsions. *J. Colloid Interface Sci.* **2013**, *403*, 1–6.
- (15) Lu, N.; Li, Z. In *Quantum Simulations of Materials and Biological Systems*; Zeng, J., Zhang, R.-Q., Treutlein, H. R., Eds.; Springer: Berlin, 2012; Chapter Graphene Oxide: Theoretical Perspectives, pp 69–84.
- (16) Marcano, D. C.; Kosynkin, D. V.; Berlin, J. M.; Sinitskii, A.; Sun, Z.; Slesarev, A.; Alemany, L. B.; Lu, W.; Tour, J. M. Improved Synthesis of Graphene Oxide. *ACS Nano* **2010**, *4*, 4806–4814.
- (17) Whitby, R. D. L.; Korobeinyk, A.; Gun'ko, V. M.; Busquets, R.; Cundy, A. B.; Laszlo, K.; Skubisewska-Zieba, J.; Leboda, R.; Tombacz, E.; Toth, I. Y.; et al. pH-driven Physicochemical Conformational Changes of Single-Layer Graphene Oxide. *Chem. Commun.* **2011**, *47*, 9645–9647.
- (18) Hunter, R. J. *Foundations of Colloid Science*, 2nd ed.; Oxford University Press: Oxford, 2001.
- (19) Fernandez-Merino, M. J.; Guardia, L.; Paredes, J. I.; Villar-Rodil, S.; Solis-Fernandez, P.; Martinez-Alonso, A.; Tascon, J. M. D. Vitamin C is an Ideal Substitute for Hydrazine in the Reduction of Graphene Oxide. *J. Phys. Chem. C* **2010**, *114*, 6426–6432.
- (20) Giesbers, M.; Kleijn, J. M.; Cohen Stuart, M. A. The Electrical Double Layer on Gold Probed by Electrokinetic and Surface Force Measurements. *J. Colloid Interface Sci.* **2002**, *248*, 88–95.
- (21) Tabor, R. F.; Morfa, A. J.; Grieser, F.; Chan, D. Y. C.; Dagastine, R. R. The Effect of Gold Oxide in Measurements of Colloidal Forces. *Langmuir* **2011**, *27*, 6026–6030.
- (22) Creux, P.; Lachaise, J.; Graciaa, A.; Beattie, J. K.; Djerdjev, A. Strong Specific Hydroxide Ion Binding at the Pristine Oil/Water and Air/Water Interfaces. *J. Phys. Chem. B* **2009**, *113*, 14146–14150.
- (23) Tabor, R. F.; Wu, C.; Lockie, H.; Manica, R.; Chan, D. Y. C.; Grieser, F.; Dagastine, R. R. Homo- and Hetero-Interactions between Air Bubbles and Oil Droplets Measured by Atomic Force Microscopy. *Soft Matter* **2011**, *7*, 8977–8983.
- (24) Israelachvili, J. N. *Intermolecular and Surface Forces*; Academic Press: San Diego, 1991.
- (25) Tabor, R. F.; Wu, C.; Grieser, F.; Dagastine, R. R.; Chan, D. Y. C. Measurement of the Hydrophobic Force in a Soft Matter System. *J. Phys. Chem. Lett.* **2013**, *4*, 3872–3877.
- (26) Tabor, R. F.; Grieser, F.; Dagastine, R. R.; Chan, D. Y. C. Measurement and Analysis of Forces in Bubble and Droplet Systems using AFM. *J. Colloid Interface Sci.* **2012**, *371*, 1–14.
- (27) Vakarelski, I. U.; Manica, R.; Tang, X.; O'Shea, S. J.; Stevens, G. W.; Grieser, F.; Dagastine, R. R.; Chan, D. Y. C. Dynamic Interactions between Microbubbles in Water. *Proc. Natl. Acad. Sci. U. S. A.* **2010**, *107*, 11177–11182.
- (28) Hutter, J. L.; Bechhoefer, J. Calibration of Atomic Force Microscope Tips. *Rev. Sci. Instrum.* **1993**, *64*, 1868–1873.

- (29) Chan, D. Y. C.; Manica, R.; Klaseboer, E. Film Drainage and Coalescence between Deformable Drops and Bubbles. *Soft Matter* **2011**, *7*, 2235–2264.